

Elastic properties of carbon nanotubes under hydrostatic pressure

S. Reich and C. Thomsen

Institut für Festkörperphysik, Technische Universität Berlin, Hardenbergstrasse 36, 10623 Berlin, Germany

P. Ordejón

Institut de Ciència de Materials de Barcelona (CSIC), Campus de la U.A.B. E-08193 Bellaterra, Barcelona, Spain

(Received 15 November 2001; published 3 April 2002)

We present first-principles calculations of the bulk and linear moduli of carbon nanotube bundles and individual tubes. The calculations were done using the local-density approximation of density-functional theory. We found the bundle bulk modulus (37 GPa) to be essentially the same as that of graphite (between 34 and 42 GPa experimentally). The elastic properties of the individual tubes in the bundles are excellently described by the elastic continuum approximation. The linear modulus along the nanotube axis is 1.5–2 higher than the radial modulus for nanotube radii between 0.8 and 1.4 nm.

DOI: 10.1103/PhysRevB.65.153407

PACS number(s): 62.20.Dc, 61.50.Ah, 64.30.+t

The elastic properties of carbon nanotubes were widely studied both for promising application, e.g., in composite nanotube materials, and to gain a better understanding of this one-dimensional carbon based material. Experimentally, uniaxial and hydrostatic stresses were realized and investigated, e.g., by x ray, transport, and optical-absorption measurements and Raman scattering.^{1–4} Theoretical studies concentrated on the evaluation of Young's modulus and Poisson's ratio, which are the most interesting elastic constants for application.^{5–9} After first reports of an unusually high Young's modulus, a value around 1 TPa, i.e., close to graphite, is now commonly accepted. The bulk modulus of carbon nanotube bundles was predicted to be 35–40 TPa by a force constants calculation, in good agreement with x-ray experiments.^{10,12} For isolated tubes or the individual tubes in a bundle, however, the calculated bulk moduli show considerable scatter. For nanotubes with a diameter $d \approx 1.4$ nm bulk moduli ranging from 130 GPa in a tight-binding molecular-dynamics simulations¹¹ to 260 GPa in a force-constant model^{5,6} were reported. A similar discrepancy was found for the linear compressibilities along the radial direction and parallel to the tube axis in this highly anisotropic material (see the compilation in Table II of Ref. 12).

Here we report an *ab initio* calculation of carbon nanotube bundles under hydrostatic stress. The volume of the bundle unit cell shows a sublinear pressure dependence with a bulk modulus of $B_0^b = 37$ GPa. The individual tubes within the bundle are ≈ 6 times stiffer ($B_0^t = 230$ GPa for tubes with $d = 8$ Å). We show that our results for the individual tubes are very well described by the elastic continuum approximation.

We simulate the structure of nanotube bundles using three-dimensional crystalline arrays of identical nanotubes arranged in a hexagonal two-dimensional (2D) lattice. The tubes are therefore of infinite length and not capped. This is a good approximation to the real bundles in which the nanotubes are of finite but very long length and the number of tubes forming the bundle is large. Calculations of (6,6), (10,0), and (8,4) nanotube bundles were performed with the SIESTA¹³ code within the local-density approximation (LDA) parametrized as by Perdew and Zunger.¹⁴ Nonlocal norm-

conserving pseudopotentials¹⁵ replaced the core electrons. The valence wave functions were described by a double- ζ polarized basis set of localized orbitals with cutoff radii of 5.12 a.u. for the *s* and 6.25 a.u. for the *p* and *d* orbitals as obtained using an energy shift of 50 meV.¹⁶ Real space integration was performed on a grid corresponding to a cutoff of ≈ 240 Ry. In the (6,6) armchair bundle we included 64 special *k* points in the calculation, 40 for the (10,0), and only the Γ point in the bundle of chiral (8,4) nanotubes. The bundle unit cell and the atomic positions were relaxed for each pressure point between 0 and 8.5 GPa by a conjugate gradient minimization under the constraint of a hydrostatic stress tensor. The relaxation was considered to be converged when all components of the stress tensor were ≈ 5 –10% within the required value (tolerances between 0.02 GPa at 0.25 GPa pressure and 0.45 GPa at 8 GPa pressure) and the forces on the atoms < 0.04 eV/Å. At zero pressure the equilibrium structure of the individual tubes in the bundle agreed to within 1% with the values expected for an ideal graphene cylinder. For comparison we also calculated graphite and graphene and found an in-plane lattice constant of 2.465 Å, which agrees well with the experiment (2.461 Å). We obtain a cohesive energy for graphene of 8.66 eV/atom, in good agreement with previous pseudopotential plane waves¹⁷ and all-electron¹⁸ calculations (8.80 and 8.87 eV, respectively). The stacking energy of the graphite planes in our calculation is 0.025 eV/atom (after correcting for basis set superposition errors), also in very good agreement with previous LDA results.¹⁷ A more complete description of the parameters and the equilibrium structure at zero pressure can be found in Ref. 19.

The equilibrium lattice constant *b* for the unit cells of the (6,6), (10,0), and (8,4) nanotube bundles varied between 11.00 and 11.43 Å for radii between 3.92 and 4.11 Å. This corresponds to a wall-to-wall distance between the tubes in a bundle of 3.1 Å, slightly lower than in graphite (3.3 Å in our calculation). The same wall-to-wall distance was obtained by Tang *et al.*¹ in a combination of x-ray experiments and a calculation based on elasticity theory.

In Fig. 1 we present the pressure dependence of the volume of the nanotube unit cell (bundle unit cell) and of the

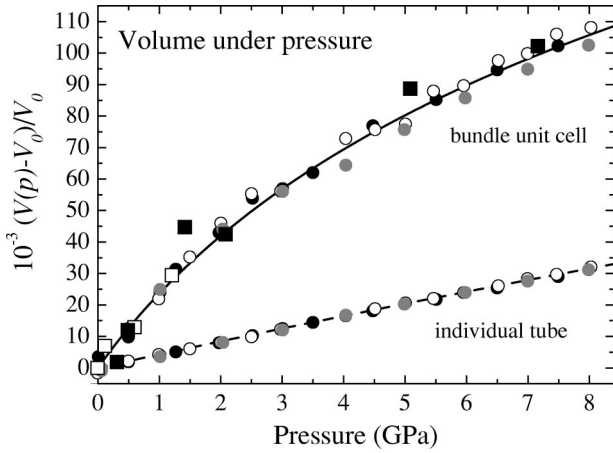


FIG. 1. Normalized volume change of the unit cell of nanotube bundles (bundle unit cell) and of the individual tubes within the bundles (individual tube) under pressure. Closed black dots correspond to (6,6) nanotubes, open dots to (10,0) tubes, and closed gray dots to (8,4) nanotubes. The closed and open square are the experimental values of Tang *et al.*¹ and Sharma *et al.*,² respectively. The lines were obtained from fits to the calculated total energy using the universal equation of state by Vinet *et al.*²⁰

individual tubes in the bundle (individual tube). The dots show the calculated results for the three bundles of tubes (see figure caption). The squares were obtained from the x-ray measurements of the bundle lattice constants in Refs. 1 and 2 assuming that the lattice constant along the z axis is not changed by the applied hydrostatic pressure. The agreement between theory and experiment is excellent. The volume of the nanotube unit cell shows a sublinear pressure dependence; from a fit with the universal equation of states²⁰ we find the bulk modulus $B_0^b = 37$ GPa and its first derivative $B_b' = 11$. Our calculated moduli of graphite are practically the same as those of the nanotube bundles (see Table I). The graphite bulk moduli reported in the literature scatter considerably; two experimental results and an all-electron calculation are included in the table for comparison. The nanotube bulk modulus we obtained is more than twice as large as that obtained from force constants calculations by Lu,⁶ similar

TABLE I. Calculated and measured bulk modulus B_0 and its first derivative at zero pressure B' of graphite and graphene compared to the calculated elastic properties of carbon nanotubes.

	B_0 (GPa)	B'	V_0 (\AA^3)
Graphite			
This work	39	10	34.961
LDA (LCGTO ^a), Ref. 18	38.8	8.3	35.204
X ray, Ref. 21	42	9.5	35.152
X ray, Ref. 22	33.8	8.9	35.12
Graphene (2D)	700	1	6.076
Nanotubes			
Bundle	37	11	
Individual	230	4.5	

^aLinear combinations of Gaussian-type orbitals.

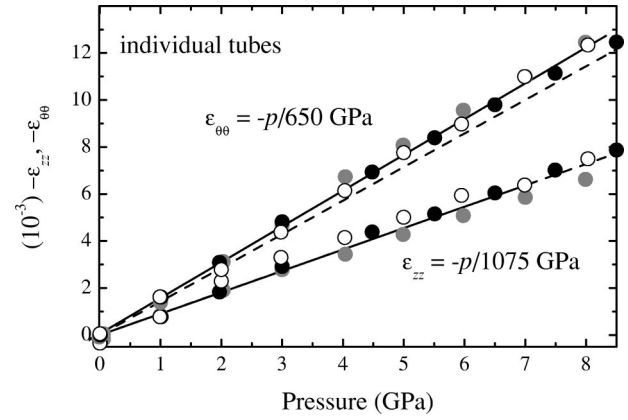


FIG. 2. Calculated radial or circumferential ($\epsilon_{\theta\theta}$) and axial strain (ϵ_{zz}) for the individual tubes in a nanotube bundle under hydrostatic pressure. The (6,6) nanotubes are shown by the black dots, (10,0) tubes by open dots, and (8,4) tubes by gray dots. The linear dependence of the two strains on pressure is shown by the full lines; the broken lines are the result of the elastic continuum model. For ϵ_{zz} the two lines coincide, therefore, the result of the *ab initio* calculation is only shown for $p < 7$ GPa.

calculations by Popov *et al.*¹⁰ are, however, in very good agreement with the *ab initio* result. The nanotubes calculated with the first-principles method have a diameter of only 8 \AA , whereas the experiments were performed on ≈ 15 \AA diameter tubes. Popov *et al.*¹⁰ predicted a dependence of the bulk modulus on the diameters of the bundled tubes between $d=0$ and 60 \AA , which peaked at $d=12$ \AA with $B_0^b = 38$ GPa. Since the diameter range between 10 and 16 \AA covers almost all single-walled nanotubes found in real samples, the bulk modulus varies only little for the particular tubes under study in experiments.

Up to now, we discussed only the dependence of the bundle unit cell on pressure. In Fig. 1 also the volume change for the individual (6,6), (10,0), and (8,4) tubes in the bundle is shown (lower trace). To find the volume of the individual tubes under pressure we assumed the nanotubes to have a cylindrical shape, i.e., $V(p) = \pi r^2(p)a(p)$. We use the axial lattice constant $a(p)$ found from the conjugate gradient minimization and as the radius $r(p)$ the mean distance of all carbon atoms from the center of the tube. This approach neglects a small hexagonal distortion of the circular cross section, which, however, even for the highest pressure points was below 5% of $r(p)$. All three nanotubes show the same pressure dependence in Fig. 1 regardless of their chirality. The pressure slope is found to be almost linear, with a bulk modulus $B_0^t = 230$ GPa, see Table I. The corresponding value of two-dimensional graphene is about three times higher.

The discrepancy between the nanotube and the graphene value can be understood when the cylindrical shape of the tubes is properly taken into account. The highly uniaxial structure of the tube yields a higher linear compressibility in the radial than in the axial direction. In Fig. 2 we show the radial ($\epsilon_{\theta\theta}$) and the axial (ϵ_{zz}) deformation of the nanotubes under applied hydrostatic pressure. At a given pressure the radial or circumferential strain is always larger than the axial strain. From Fig. 2 we find the axial M_z^t and radial M_θ^t linear moduli,

TABLE II. Linear moduli calculated for the individual nanotubes by first-principles methods and within elasticity theory. The *ab initio* value for graphite is given for comparison. All moduli are in GPa.

	$M_z = -(d \ln a/dp)^{-1}$	$M_\theta = -(d \ln r/dp)^{-1}$
Nanotubes		
<i>Ab initio</i> ($d=8$ Å)	1075	650
Elasticity ($d=8$ Å)	1100	750
Elasticity ($d=14$ Å)	930	490
Graphite (<i>ab initio</i>)	1410	

$$M_z^t = - \left[\frac{d \ln a(p)}{dp} \right]^{-1} = 1075 \text{ GPa} \quad (1)$$

and

$$M_\theta^t = - \left[\frac{d \ln r(p)}{dp} \right]^{-1} = 650 \text{ GPa.} \quad (2)$$

Whereas M_z^t is similar to the graphite in-plane modulus (1410 GPa in our calculation, see Table II), the compressibility in the radial direction M_θ^{-1} is much larger.

To separate the geometrical part of the pressure dependence, i.e., the cylindrical shape, from additional contributions we calculate the two moduli within a continuum model. Consider a nanotube as a rolled up hollow cylinder with a finite wall thickness made out of graphene. Within elasticity theory M_z^e and M_θ^e are then obtained as²³

$$M_z^e = \frac{E}{1-2\nu} \frac{R_o^2 - R_i^2}{R_o^2}, \quad (3)$$

$$M_\theta^e = \frac{E}{1-2\nu} \frac{R_o^2 - R_i^2}{R_o^2} \left(1 + \frac{1+\nu}{1-2\nu} \frac{R_i^2}{r^2} \right)^{-1}, \quad (4)$$

where E is Young's modulus, ν is Poisson's ratio, r is the nanotube radius, and R_o and R_i are the inner and outer radii of the cylinder. Possible choices for r , R_i , and R_o in a given tube and the dependence of the moduli on these values were discussed in Ref. 23. We used the mean radius $r=4$ Å as calculated for the (6,6), (8,4), and (10,0) tube at ambient pressure; the inner and outer radii are given by subtracting or adding half of the wall-to-wall distance between the tubes in the bundle (3.1 Å in our calculation). We then obtain ($E=1$ TPa and $\nu=0.14$)²³ the broken lines in Fig. 2 (compare also Table II). They are in excellent agreement with the *ab initio* result showing that the elastic response is well ex-

plained by the nanotube's cylindrical shape. In particular, the continuum model also implies that the elastic properties of the nanotubes are insensitive to their chirality, which we also found in the *ab initio* calculations. It is quite surprising that a continuum model accurately describes the elastic properties of a system constructed from only a single monolayer. In two-dimensional semiconductors a similarly wide range of validity was found by Bernard and Zunger.²⁴

An interesting point currently under controversial debate is a structural phase transition in nanotubes under pressure. It was proposed by Peters *et al.*²⁵ that the tube's cross section collapses to an oval shape under pressure to explain the disappearance of the radial breathing mode in high-pressure Raman spectra around ≈ 2 GPa. Tang *et al.*¹ concluded similarly on the basis of x-ray measurements, whereas Sharma *et al.*² stressed that the triangular lattice persisted up to 10 GPa in their measurements. In the *ab initio* calculation we found a small hexagonal distortion of all tubes when bundled. It slowly increased with increasing pressure, but even for $p=8.5$ GPa remained below 5%. At even higher pressure (≈ 10 GPa) the armchair nanotubes collapsed to flat ellipses. The elliptical structure might be preferred at high pressure because the volume inside the tubes is much reduced compared to the circular cross section, but it requires a strong bending of the nanotube's wall. We currently investigate whether the same behavior is found in the other tubes as well. For a comparison with experiment, however, we need to calculate larger diameter ($d \approx 14$ Å) nanotubes, which will be the subject of a future work.

In conclusion, we studied the elastic response of carbon nanotube bundles to hydrostatic pressures up to 8.5 GPa. The bulk modulus of the bundles was found to be 37 GPa, the same value as in graphite. For the individual tubes in the bundle an elastic continuum model is in excellent agreement with our *ab initio* calculation. Based on the continuum approximation we can estimate the bulk modulus in typical nanotubes ($d \approx 14$ Å) as 200 GPa and the linear compressibility in the radial and axial direction as 490 GPa and 930 GPa, respectively.

ACKNOWLEDGMENTS

We acknowledge support from the Ministerio de Ciencia y Tecnología (Spain) and the DAAD (Germany) for a Spanish-German Research action (HA 1999-0118). P. O. acknowledges support from Fundación Ramón Areces (Spain), EU project SATURN IST-1999-10593, and Spain-DGI project BFM2000-1312-002-01. This work was partly supported by the Deutsche Forschungsgemeinschaft under Grant No. Th 662/8-1.

¹J. Tang, L.-C. Qin, T. Sasaki, M. Yudasaka, A. Matsushita, and S. Iijima, Phys. Rev. Lett. **85**, 1887 (2000).

²S.M. Sharma, S. Karmakar, S.K. Sikka, P.V. Teredesai, A.K. Sood, A. Govindaraj, and C.N.R. Rao, Phys. Rev. B **63**, 205417 (2001).

³R. Gaál, J.-P. Salvetat, and L. Forró, Phys. Rev. B **61**, 7320 (2000).

⁴U.D. Venkateswaran, E.A. Brandsen, U. Schlecht, A.M. Rao, E. Richter, I. Loa, K. Syassen, and P.C. Eklund, Phys. Status Solidi B **223**, 225 (2001).

- ⁵J.P. Lu, *J. Phys. Chem. Solids* **58**, 1649 (1997).
- ⁶J. Lu, *Phys. Rev. Lett.* **79**, 1297 (1997).
- ⁷E. Hernández, C. Goze, and A. Rubio, *Appl. Phys. A: Mater. Sci. Process.* **68**, 287 (1999).
- ⁸D. Sánchez-Portal, E. Artacho, J.M. Soler, A. Rubio, and P. Ordejón, *Phys. Rev. B* **59**, 12 678 (1999).
- ⁹G.V. Lier, C.V. Alsenoy, V.V. Doren, and P. Geerlings, *Chem. Phys. Lett.* **326**, 181 (2000), and references therein.
- ¹⁰V. Popov, V.V. Doren, and M. Balkanski, *Solid State Commun.* **114**, 395 (2000).
- ¹¹U.D. Venkateswaran, A.M. Rao, E. Richter, M. Menon, A. Rinzler, R.E. Smalley, and P.C. Eklund, *Phys. Rev. B* **59**, 10 928 (1999).
- ¹²S. Reich, H. Jantoljak, and C. Thomsen, *Phys. Rev. B* **61**, R13 389 (2000).
- ¹³D. Sanchez-Portal, P. Ordejón, E. Artacho, and J.M. Soler, *Int. J. Quantum Chem.* **65**, 453 (1997).
- ¹⁴J.P. Perdew and A. Zunger, *Phys. Rev. B* **23**, 5048 (1981).
- ¹⁵N. Troullier and J.L. Martins, *Phys. Rev. B* **43**, 1993 (1991).
- ¹⁶E. Artacho, D. Sánchez-Portal, P. Ordejón, A. García, and J. Soler, *Phys. Status Solidi B* **215**, 809 (1999).
- ¹⁷M.C. Schabel and J.L. Martins, *Phys. Rev. B* **46**, 7185 (1992).
- ¹⁸J.C. Boettger, *Phys. Rev. B* **55**, 11 202 (1997).
- ¹⁹S. Reich, C. Thomsen, and P. Ordejón, *Phys. Rev. B* **64**, 195416 (2001).
- ²⁰P. Vinet, J.H. Rose, J. Ferrantes, and J.R. Smith, *J. Phys.: Condens. Matter* **1**, 1941 (1989).
- ²¹Y.X. Zhao and I.L. Spain, *Phys. Rev. B* **40**, 993 (1989).
- ²²M. Hanfland, H. Beister, and K. Syassen, *Phys. Rev. B* **39**, 12 598 (1989).
- ²³C. Thomsen, S. Reich, H. Jantoljak, I. Loa, K. Syassen, M. Burghard, G.S. Duesberg, and S. Roth, *Appl. Phys. A: Mater. Sci. Process.* **69**, 309 (1999).
- ²⁴J. Bernard and A. Zunger, *Appl. Phys. Lett.* **65**, 165 (1994).
- ²⁵M.J. Peters, L.E. McNeila, J.P. Lu, and D. Kahn, *Phys. Rev. B* **61**, 5939 (2000).